scientific reports

Check for updates

OPEN

Evaluation of blood MSI burden dynamics to trace immune checkpoint inhibitor therapy efficacy through the course of treatment

Egor Veselovsky[1,2], Alexandra Lebedeva[1,3], Olesya Kuznetsova[1,4], Daria Kravchuk[5], Ekaterina Belova[1,3,6], Anastasia Taraskina[1], Tatiana Grigoreva[1,3], Alexandra Kavun[1], Victoria Yudina[4], Laima Belyaeva[1,3], Vladislav Nikulin[4], Vladislav Mileyko[1,3], Alexey Tryakin[4], Mikhail Fedyanin[4,5,7] & Maxim Ivanov[1,3]✉

Analysis of serial liquid biopsy (LB) samples has been found to be a promising approach for the monitoring of tumor dynamics in the course of therapy for patients with colorectal cancer (CRC). Currently, somatic mutations are used for tracing the dynamics of the tumor via LB. However, the analysis of the dynamic changes in the molecular signatures such as microsatellite instability (MSI) is not currently used. We hypothesized that changes in blood MSI burden (bMSI) could be registered using serial LB sampling in the course of immune checkpoint inhibitors (ICI), and that its changes could potentially correlate with treatment outcomes. We report the preliminary findings of the observational trial launched to study (NCT06414304) the dynamics of bMSI in 9 MSI-positive CRC patients receiving ICI. NGS-based MSI testing was performed on both pre-treatment FFPE and serial LB samples. For patients who had detectable bMSI burden in any of the LB samples ($n = 8$, 89%), median bMSI was 1.4% (range, 0.01-40%). Among patients with detectable MSI in available FFPE samples, median MSI burden was 29.3% (range, 10–40%). bMSI detected in baseline LB and FFPE samples were positively correlated (Pearson's R 0.47). Maximal variant allele frequencies of driver mutations observed in LB were also positively correlated with bMSI burden (Pearson's R 0.7). Patients who had clinical benefit had undetectable bMSI burden at follow-up. Our results provide the rationale for further validation of bMSI as a predictive biomarker of ICI in MSI-positive patients.

Keywords Microsatellite instability, Colorectal cancer, Next-generation sequencing, Immunotherapy, Liquid biopsy, Immune checkpoint inhibitors

Abbreviations

LB	Liquid biopsy
CRC	Colorectal cancer
MSI	Microsatellite instability
bMSI	Blood MSI burden
ICI	Immune checkpoint inhibitors
IT	Immunotherapy

[1]OncoAtlas LLC, 4/1A, Leninskiy Prospect, Moscow, Russian Federation119049. [2]Department of Evolutionary Genetics of Development, Koltzov Institute of Developmental Biology of the Russian Academy of Sciences, Moscow, Russian Federation. [3]Sechenov First Moscow State Medical University, Moscow, Russian Federation. [4]Federal State Budgetary Institution N.N. Blokhin National Medical Research Center of Oncology, Moscow, Russian Federation. [5]State Budgetary Institution of Health Care of the City of Moscow "Moscow Multidisciplinary Clinical Center" "Kommunarka" of the Department of Health of the City of Moscow, Moscow, Russian Federation. [6]Lomonosov Moscow State University, Moscow, Russian Federation. [7]Federal State Budgetary Institution "National Medical and Surgical Center named after N.I. Pirogov" of the Ministry of Health of the Russian Federation, Moscow, Russian Federation. ✉email: maxim.ivanov@oncoatlas.ru

dMMR	Mismatch repair deficiency
PCR	Polymerase chain reaction
IHC	Immunohistochemistry
NGS	Next-generation sequencing
ctDNA	Circulating tumor DNA
VAF	Variant allele frequency
STR	Short tandem repeat
RECIST v1.1	Response Evaluation Criteria in Solid Tumor version 1.1
ECOG	Eastern Cooperative Oncology Group
FFPE	Formalin-fixed paraffin-embedded
VUS	Variant of uncertain significance
CR	Complete response
PR	Partial response
SD	Stable disease
PD	Disease progression
pCR	Complete pathological response
mPR	Major pathological response
N/A	Not available
MSS	Microsatellite stable
wt	Wild type
BL	Baseline blood plasma sample
CT	Computed tomography

Background

Colorectal cancer (CRC) remains one of the leading causes of cancer-related mortality globally[1]. Although most patients are diagnosed with early-stage disease, the 5-year survival rate is 71%[2]. Notwithstanding the advancements in screening, diagnosis, and treatment modalities, there is still an ongoing need for innovative approaches to improve patient outcomes.

Immunotherapy (IT) with immune checkpoint inhibitors (ICI) has emerged as promising treatment for CRC[3]. However, ICI have only demonstrated efficacy in microsatellite instability (MSI) or mismatch repair deficiency (dMMR) positive CRC[4]. In stage IV CRC, the frequency of MSI is relatively low, at 4%, compared to 10–20% in stages I-III[5,6], allowing IT to become the preferred strategy in the early stages[7].

MSI can be associated with Lynch syndrome[8–10], however, in CRC, most cases of MSI are sporadic, arising from frequently co-occurring epigenetic inactivation of MLH1 and BRAF V600E mutations[11–13], found in up to 45% of CRC with sporadic MSI[14,15].

The standard methods for assessing MSI and dMMR are polymerase chain reaction (PCR) and 4-antibody immunohistochemistry (IHC). In clinical practice, limitations of MSI/dMMR testing include false negative or false positive results in cases when the sample quality is suboptimal, as well as variable concordance between the two methods. Furthermore, IHC can yield inconclusive results, such as the loss of only one protein[9,16]. Next-generation sequencing (NGS) is an emerging approach that allows to expand the range of analyzed markers[9]. NGS allows to dynamically monitor tumor variability through the analysis of mutations in circulating tumor DNA (ctDNA)[17,18]. NGS-based analysis of liquid biopsy (LB) has several advantages, as it allows to evaluate the dynamics of tumor variability, as well as monitor the response to therapy[19]. There is a discrepancy in assessing patient responses to therapy using ctDNA. Current approaches are based on an evaluation of total variant allele frequency (VAF) or ctDNA copies per mL of plasma or VAF of the driver mutation.

The literature encompasses findings on MSI assessment in ctDNA through high-throughput sequencing employing diverse methodologies[20–22]. The majority of computational NGS-based approaches for MSI analysis rely on the classification of each single short tandem repeat (STR) on stable/unstable with further accumulation of MSI score as the percent of unstable loci[23]. Numerous studies demonstrated outstanding sensitivity of diverse software utilizing this approach for detecting MSI in tumor and/or LB samples. Nevertheless, per-STR binary classification puts an intrinsic restraint on the use of tracing MSI score dynamics throughout longitudinal monitoring of LB, as the score reflects the breadth of instability across STRs rather than the burden thereof in DNA fragments derived from exhibiting intra-tumor heterogeneity and contamination with normal tissue[24].

In order to investigate dynamics of bMSI of CRC patients receiving ICI's, we initiated a multicenter observational clinical trial. Here, we describe outcomes of the first nine patients enrolled in the study.

Methods

Ethics statement

The study was approved by the Ethics Committee at the Blokhin National Medical Research Center of Oncology Research Center (№13-02-2023) and was carried out in accordance with the Declaration of Helsinki. Written informed consents were received from the patients before starting any procedures related to the study.

Study design and participants

This is a prospective multicenter observational study (ClinicalTrials ID: NCT06414304) evaluating the dynamics of MSI burden in serial LB samples from patients receiving ICI due to the presence of MSI/dMMR.

Eligible patients were aged ≥ 18 years with MSI/dMMR-positive confirmed colorectal adenocarcinoma with measurable disease as per Response Evaluation Criteria in Solid Tumor version 1.1 (RECIST v1.1) by local

investigator/radiology assessment, Eastern Cooperative Oncology Group (ECOG) performance status of 0 or 1, and adequate organ function were eligible for the study. Patients had to be candidates for the treatment with ICI regardless of the setting. Patients not willing or unable to participate in blood plasma collection were also excluded.

Participants described here underwent treatment and study related procedures at the N.N. Blokhin National Medical Research Center or Moscow Multidisciplinary Clinical Center "Kommunarka" (Moscow, Russia) from 2022 to 2024. Patients received prolgolimab (anti-PD-1 monoclonal antibody[25]) in neoadjuvant settings under investigational protocol or nivolumab for the systemic treatment of metastatic disease.

Medical records including radiological and pathological response data were collected for all patients.

Collection of clinical samples and diagnostic procedures

Participants had to provide archival formalin-fixed paraffin-embedded (FFPE) blocks ('tumor baseline') and a blood plasma ('blood baseline' or 'BL') sample derived prior to the start of ICI. Additionally, blood plasma samples were collected two (W2) and four weeks (W4) following the initiation of ICI, as well as at every control visit (F1 and F2).

As part of the study, patients underwent confirmatory MSI/dMMR testing and NGS analysis of primary tumor samples and all serial LB samples.

Venous blood samples were collected into 10 mL EDTA tubes (GradBioMed, Russia). The tubes were stored at room temperature and transferred to the laboratory within 5 days.

MSI testing

Confirmatory MSI/dMMR testing with gold standard methods (5-loci PCR or 4-antibody IHC was performed, depending on the preceding method used prior to the study recruitment), on primary FFPE samples. In cases when initial MSI testing was performed via NGS, both PCR and IHC were used. In cases when IHC resulted in the loss of only two of the four MMR proteins, the result was considered equivocal as per ESMO guidelines[9].

NGS-based MSI testing was performed on both FFPE and serial LB samples.

DNA extraction and sequencing

Tumor DNA was isolated from archival FFPE blocks using the ExtractDNA FFPE kit (Evrogen JSC, Russia) according to the manufacturer's protocol.

Blood plasma samples were centrifuged for 15 min at 1900 g and 4 °C. The supernatants were collected and centrifuged for 10 min at 16,000 g and 4 °C, and were then stored at -80 °C. ctDNA from blood plasma was isolated using the QIAamp MinElute ccfDNA Midi Kit (Qiagen, Hilden, Germany). DNA was quantified using the Qubit 2.0 fluorometer and the Qubit dsDNA HS Assay kit (Thermo Fisher Scientific, Inc., Waltham, MA, USA) according to the manufacturer's protocol.

Amplification of target regions was performed using the Solo-test Atlas Pro (OncoAtlas LLC, Russia) panel covering clinically significant regions of 38 commonly altered genes (SNV, indel, CNV) in cancer, not including Lynch syndrome genes, as well as 56 STRs for MSI detection. Pooled libraries were sequenced employing Genolab sequencer (GeneMind Biosciences, China).

Sequence data analysis was conducted as described previously[26,27]. In short, reads were aligned to the human genome assembly GRCh37.p13. Samtools was employed to conduct an initial assessment of the technical properties of the identified variants, including variant site coverage depth, observed alternative allele counts, observed alternative allele frequency[28]. Additional technical annotations of detected variants were performed using FreeBayes[29], Mutect2[30], SGA[31], and SiNVICT[32]. MSIsensor2 was used to call count of unstable STRs[33]. MSI burden was calculated as cumulative prevalence of k-mers corresponding to altered STR across all STRs within a single sample[34]. Data analysis (including variant calling and MSI analysis) was conducted within Solo AVES platform tailored to Solo-test Atlas Pro panel (validation studies will be published separately) and provided by test-kit supplier. Variant calling, VAF calculation, MSI detection and bMSI fraction calculation were additionally validated prior to the current serial case report using the mixing experiments of the paired samples (Supplementary table S1, Supplementary Fig. S1). Oncoprints were made with Oncoprinter[35–37].

Mutation classification

Mutations were classified as oncogenic, uncertain significance (VUS) or neutral according to community guidelines[38]. OncoKB, JAX and a proprietary database were used for the identification of driver mutations[39,40]. Neutral or VUS mutations were considered passenger.

Statistical analysis

Descriptive measures (i.e., median) were derived for continuous variables and categorical variables were expressed as % frequency distribution. Pearson correlation coefficient and Fisher's exact test were used for statistical analysis. A p value of < 0.05 was considered as significant with two-sided statistical tests. Analysis was carried out using the SciPy library for Python.

Results

Clinical characteristics and outcomes

Nine patients were recruited to the study. The patients' median age at study enrollment was 56 years (range, 28–77). Seven patients had colon cancer and 2 had rectal cancer. Most CRC patients had right-sided localization of the primary tumor (before splenic flexure), one had left-sided localization, and one was diagnosed with synchronous tumors of the ascending and sigmoid colon (Table 1). Patients who had localized disease at the time of study enrollment ($n = 7$) were assigned to the neoadjuvant treatment with prolgolimab under investigational

Patient ID	Sex	Primary tumor location	TNM	Tumor stage	Drug	Therapy setting	Method used for initial MSI/dMMR analysis	BRAF V600E status	Radiological response	Pathological response	Reason for withdrawal
Case 1	Male	Left	T3N2M0	III	Prolgolimab	Neoadjuvant	PCR	wt	PR	mPR	Completion of the planned course of treatment
Case 2	Male	Right	T4bN1M0	III	Nivolumab	Palliative	PCR	wt	SD	NA	Refusal of treatment
Case 3	Female	Right	T3N1M0	III	Prolgolimab	Neoadjuvant	PCR	V600E	Censored	NA	Death
Case 4	Female	Right/Left	T3N2Mx	III	Prolgolimab	Neoadjuvant	PCR	wt	CR	NA	Completion of the planned course of treatment
Case 5	Male	Rectum	T4N2aM0	III	Prolgolimab	Neoadjuvant	PCR	V600E	PR	NA	Completion of the planned course of treatment
Case 6	Male	Right	T3N2M0	III	Prolgolimab	Neoadjuvant	PCR	wt	PR	pCR	Completion of the planned course of treatment
Case 7	Female	Right	T3N0M0	II	Prolgolimab	Neoadjuvant	PCR	V600E*	CR	pCR	Completion of the planned course of treatment
Case 8	Male	Rectum	T4aN1bM0	III	Prolgolimab	Neoadjuvant	PCR	wt	PR	pCR	Completion of the planned course of treatment
Case 9	Male	Right	T3N1M1	IV	Nivolumab	Palliative	PCR	V600E**	PD	NA	Death

Table 1. Clinical characteristics of the first nine patients included in the clinical trial. BRAF V600E status is listed according to the patients' medical records. *For case 7, BRAF mutation was previously found by PCR, but was undetectable by NGS analysis. **For case 9, BRAF mutation was only identified via NGS described here. Abbreviations: N/A - not available, MSS - microsatellite stable, MSI - microsatellite instability, SD - stable disease, (m)PR - (major) partial response, (p)CR - (pathological) complete response, PD - progressive disease, wt - wild type, PCR - polymerase chain reaction, IHC - immunohistochemistry.

protocol. Two patients had advanced/metastatic disease and were assigned to systemic treatment with nivolumab monotherapy.

As per treatment guidelines, molecular testing of the commonly altered oncogenes in CRC had been performed prior to the study recruitment for all of the patients. According to the medical records and/or subsequent NGS FFPE and/or LB analysis, the BRAF p.V600E variant was identified in 4 patients with a median age of 64 years (range, 41–77), while other 5 patients with wild-type BRAF had a median age of 48 (range, 28–66). All patients had MSI detected by PCR. Confirmatory IHC testing was performed for 4 (44.4%) patients, as for others, no baseline FFPE was available ($n=3$), or the available FFPE sample had suboptimal tumor content ($n=2$). Results of PCR and IHC were concordant in 50% of the tested cases. Although no germline analysis was conducted, according to the medical records, no patients had a reported family or personal history of Lynch syndrome-related cancer.

Of 7 patients receiving neoadjuvant treatment, 2 (29%) had complete response (CR), 4 (57%) had partial response (PR) and 1 (14%) was censored. Of 2 patients receiving systemic therapy one had stable disease (SD) and one had disease progression (PD). Of 4 patients who underwent surgery, 3 had complete pathological response (pCR) and 1 had major pathological response (mPR).

Mutational profile and blood MSI burden analysis

Baseline FFPE samples were available for 5 (56%) at the time of analysis. Of those, 4 samples were classified as MSI-positive by NGS (80% agreement with IHC/PCR; 100% agreement with PCR) (Table S2). Among the 9 baseline LB samples, 7 (77%) were MSI-positive. Among the 5 available tumor-plasma paired samples, 4 had concordant MSI status determined by NGS (80% agreement). MSI status established in ctDNA was also concordant with the results obtained by standard methods (8 of 9, 89% agreement).

Among the 5 tumor samples mutations were detected in 4 samples. A total of 16 mutations were detected in 5 available FFPE samples, with a median number of mutations of 4 (range, 0–5). Of 9 BL samples, 7 had at least one mutation, with a total of 7 mutations identified (median, 1; range, 0–2).

During blood ctDNA monitoring (described in the section below) additional 3 mutations were detected. In summary, 21 mutations were found, 12 of them were classified as driver and 9 as passenger. The detected mutations were typical for the CRC mutational landscape, including BRAF mutations[41] (Fig. 1).

Correlation of bMSI burden with clinical responses

For most patients ($n=5$; 56%), LB samples were collected at 5 time points, while for the remaining patients, there were a median of 2.5 time points (range from 2 to 4). For 6 out of 7 patients receiving neoadjuvant therapy, sample collection was stopped due to the completion of therapy. Of 2 patients receiving treatment in the palliative setting, 1 had PD and died before F1, and 1 achieved SD and refused treatment after F2. One patient receiving neoadjuvant therapy died before reaching W4 time point and was censored (Table S2).

The dynamics of bMSI and VAF of the observed mutations were generally consistent with the patients' clinical outcomes (Fig. 2). For patients who had detectable bMSI burden in any of the LB samples ($n=8$, 89%), median bMSI burden was 1.4% (range, 0.01-40%). Among patients with detectable MSI in FFPE samples ($n=4$, 80% of available FFPE), median MSI burden was 29.3% (range, 10–40%). MSI burden detected in baseline LB

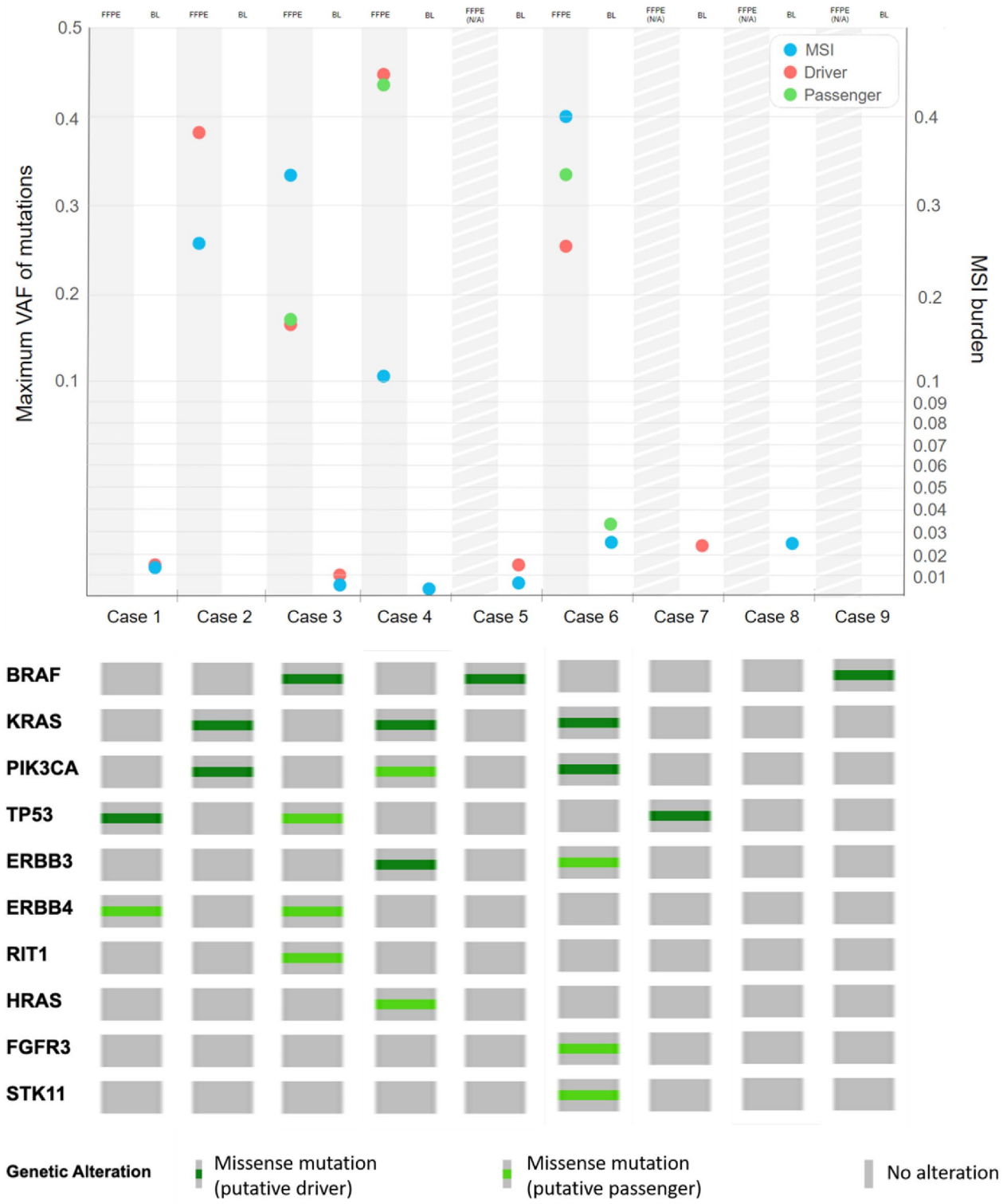

Fig. 1. Results of NGS analysis. Maximum VAF of mutations and MSI burden in baseline FFPE (when available) and baseline blood plasma (BL) samples (top) and mutations detected at any time point (i.e., in any of the patients' samples) for all of the patients included in the analysis (bottom). Abbreviations: VAF - variant allele frequency, BL - baseline blood plasma sample, FFPE N/A - FFPE not available.

(bMSI) and FFPE samples were positively correlated (Pearson's R 0.47). bMSI burden and maximal VAFs of driver mutations observed in LB were also positively correlated (Pearson's R 0.7).

For 2 patients (Cases 3, 9) who died or had PD, a clear increase of both bMSI and cumulative VAFs at available time points (W2 for Case 3, W4 for Case 9) was observed. Case 1 initially had an increase in bMSI and

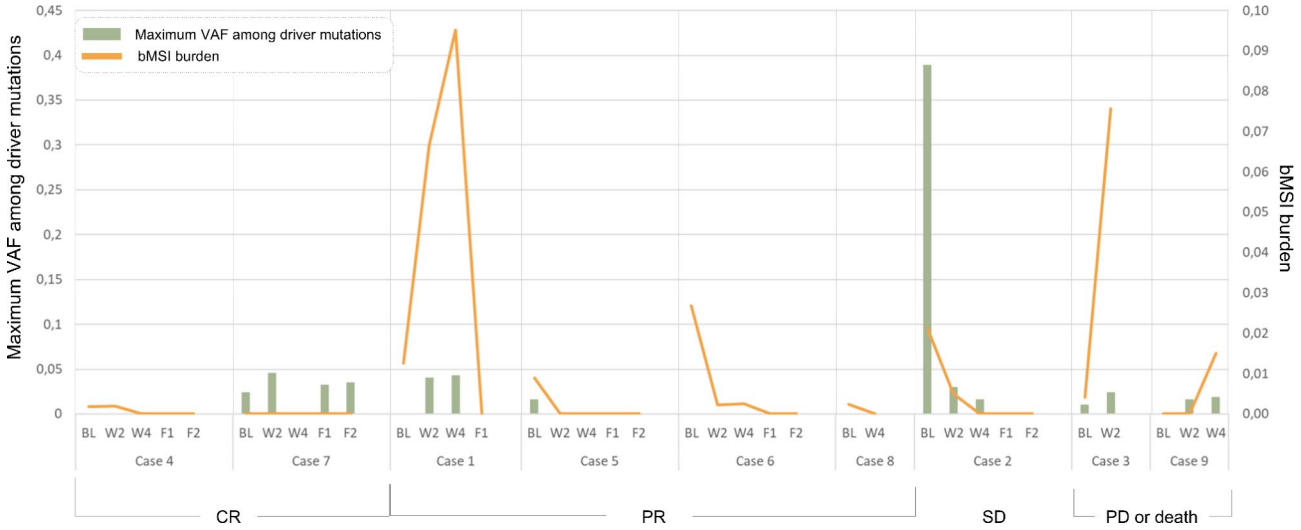

Fig. 2. Dynamics of bMSI and maximal VAF of driver mutations observed in each of the patients' serial blood plasma samples. Patient cases are grouped by the radiological responses to ICI.

VAFs at W2 (+5.4% and +4% for bMSI and maximum VAF of driver, respectively, as compared to baseline LB samples) and W4 (+2.9% and +0.23% for bMSI maxVAF of driver, respectively, as compared to W2 samples), followed by a dramatic decrease to zero values at F1 point (154th day of treatment), which was consistent with the clinical observations of a major PR. Although for Case 7 no signs of bMSI along with no decrease in the VAF of driver mutations were observed, the patient achieved a CR (radiological and pathological) to the therapy. A decrease of both bMSI and mutational VAF to zero values observed in three cases (Cases 5, 6, 8) was consistent with pCR. For Case 8, only baseline and W4 LB samples were available at the time of analysis. Overall, patients who had CR, PR or SD had undetectable bMSI burden at follow-up. Radiological and pathological responses were consistent for Cases 1, 7 (Tables S2-S3, Fig.S2).

In order to compare the dynamics of ctDNA parameters with radiological responses, contingency table analysis was performed. Pairs of computed tomography (CT) results, carried out in an interval of 1–3 months, were selected. CT results changes within pairs were stratified into 5 categories: ">20% increase", "<20% increase", "no changes", "<20% decrease", ">20% decrease". For every second CT result in a pair the closest ctDNA analysis in an interval of -3/+4 weeks was chosen. The result of ctDNA analysis was also interpreted as a change from previous analysis and also stratified into 5 groups: "increase for more than 50%", "increase for less than 50%", "no changes", "decrease for less than 50%", "decrease for more than 50%". "No changes" was determined as change less than 20%, or, for bMSI only, absolute change less than 0.1. Fisher's exact test did not reveal a statistically significant relationship between CT and ctDNA results (Fig. 3).

Discussion

Here, we describe preliminary data on the relationship between the dynamics of bMSI and mutational status dynamics following ctDNA NGS analysis and the response to anti-PD-1 IT. Patients participating in the study received IT in either the neoadjuvant setting ($n=7$, stages II/III), or as systemic therapy for metastatic disease ($n=2$, stage IV). It is considered that the release of ctDNA is contingent upon tumor burden, vascularity, and location[42]. Detecting ctDNA is hindered during the early stages of disease[43,44]. The location of metastatic sites is also thought to influence the ctDNA level[45]. Nevertheless, preliminary results of our study suggest the clinical utility of monitoring bMSI and mutational dynamics in serial LB samples in both early and late stages of CRC.

In routine clinical practice, treatment decisions are made based on the results of radiological assessments of the target lesions. However, standard imaging can miss early progression or response, and does not fully capture the changes within the tumor. Studies show that ctDNA analysis might be a suitable addition, as the appearance of ctDNA can oftentimes precede the radiological progression, and changes in ctDNA reflect the dynamic changes in the tumor in the course of therapy[46–48]. The promise of ctDNA analysis as an additional tool for monitoring therapy responses and guiding therapeutic decisions has been widely studied. For instance, in previous studies of neoadjuvant therapy, ctDNA dynamics demonstrated a better association with treatment efficacy and pathological response compared with CT in both CRC and other tumor types[19,49]. In the metastatic CRC, the rechallenge of anti-EGFR therapy can be guided by the analysis of ctDNA dynamics[50]. In breast cancer, switching to fulvestrant after the rise of ESR1 mutation in ctDNA in the course of aromatase inhibitor therapy has been shown to result in significant clinical benefit[51]. To the best of our knowledge, clinical trials are yet to clarify the role of ICI discontinuation and rechallenge in the treatment of patients with MSI-positive tumors. Nonetheless, ctDNA monitoring appears to be a promising tool aiding the identification of hyper- and pseudoprogression, a persistent clinical problem[52–54].

From a methodological point of view, current approaches for the analysis of ctDNA for monitoring tumor dynamics is based on the assessment of VAF of driver mutations[19]. Given that only a subset of MSI-positive

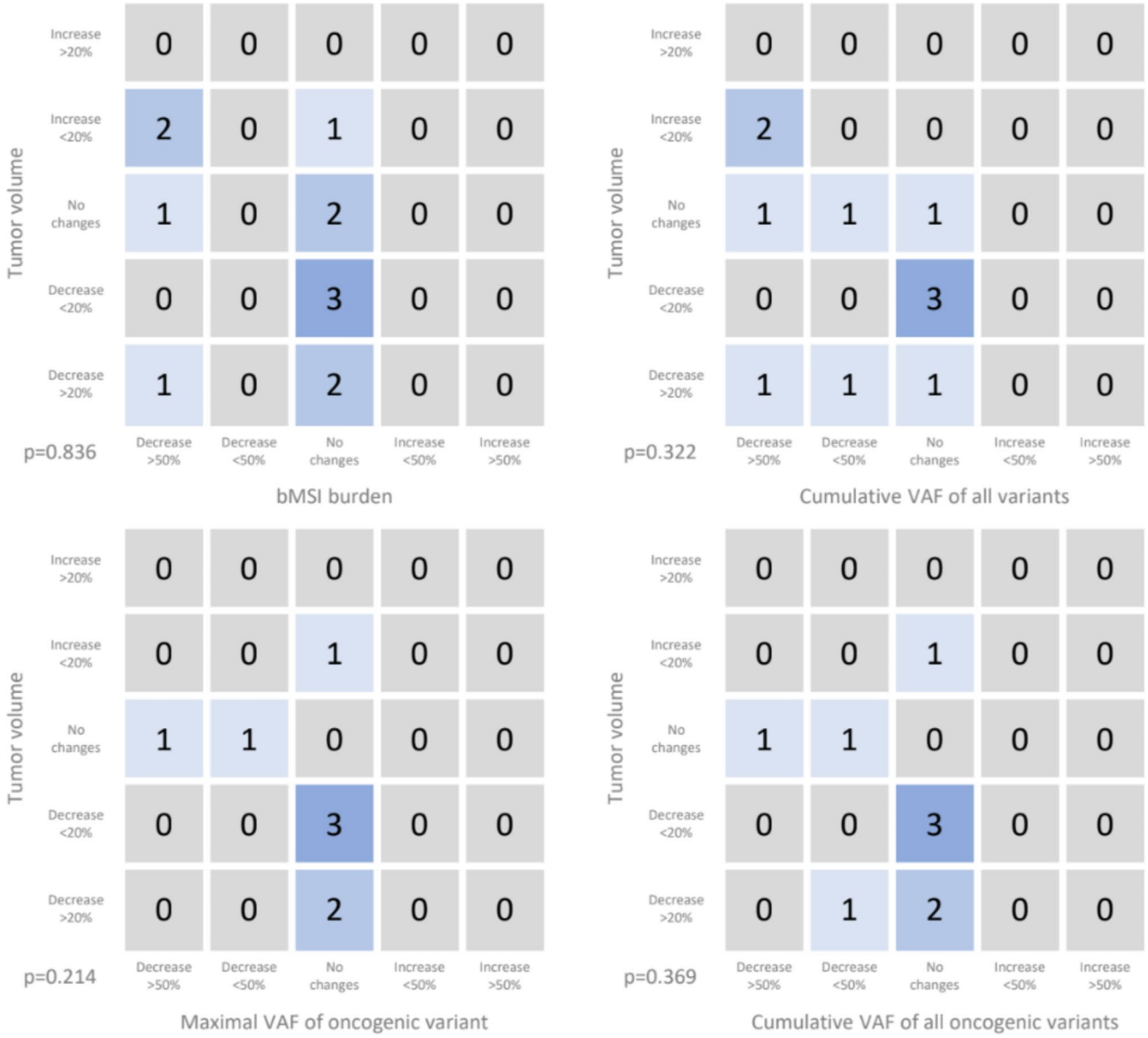

Fig. 3. Connection of tumor volume radiological changes with changes in MSI-score and VAFs in the blood plasma. One point was added to the corresponding cell of the table if the dynamics of CT and ctDNA parameters coincided. The following ctDNA parameters were used: bMSI, cumulative VAF of all variants, maximal VAF of oncogenic variant, cumulative VAF of all oncogenic variants.

tumors harbor BRAF mutations and that the molecular profiles of MSI vs. MSS tumors appear to differ[55], VAF-based evaluation of tumor changes in ctDNA might be limited. Using a different approach, such as the analysis of genomic signatures in ctDNA, may be helpful in overcoming the limitations associated with the lack of driver mutations in MSI-positive tumors. This approach has only been validated in relation to bTMB, and not bMSI. In a meta-analysis by Wei et al., bTMB was not found to be predictive of ICI benefit[56]. Given that MSI exhibits spatial and temporal heterogeneity in metastatic disease[57], we reasoned that bMSI monitoring might be an alternative approach for molecular-guided clinical decisions during the course of ICI for patients with MSI-positive tumors. Additionally, methodologically, this approach might be easier, as bMSI analysis may not require molecular barcoding.

Analysis of ctDNA allowed for accurate detection of bMSI, which was highly concordant with VAF of the observed mutations, however, bMSI analysis exhibited higher accuracy in relation to treatment outcomes. In terms of therapy response monitoring, analysis of bMSI dynamics in serial plasma samples and VAFs changes were generally consistent with response to the therapy. For patients with negative treatment outcomes, bMSI rapidly increased in the course of treatment, while for patients with clinical benefit bMSI was undetectable on the first follow-up visit after starting ICI. The only patient with undetectable level of MSI in ctDNA had stage II disease, which is consistent with observations that at earlier stages sensitivity of ctDNA tests is lowered (Case 7). Although generally correlating with the treatment outcomes, a standalone analysis of maximal VAF of driver

mutations, a methodology commonly used for the analysis of tumor dynamics using blood plasma, was not consistent with treatment outcomes for all of the patients, partially due to the fact that not all of the patients had detectable driver mutations.

Nevertheless, although unlike VAF analysis, bMSI dynamics were consistent with the results of radiological assessment in all cases (Fig. 2), the study was unable to statistically confirm the connection between dynamics of the ctDNA parameters and the dynamics of objective responses registered with CT. This may not only be due to the small sample size, but the mismatches in the testing time via CT and ctDNA. Additionally, bMSI correlated with VAF of the observed mutations in serial LB samples, indicating that determination of bMSI is highly dependent on the total ctDNA fraction. At the same time, in 3 (out of 5) cases with known pathological response, the clearance of bMSI to zero coincided with pCR (Cases 5, 6, 8), while radiological responses coincided with pathological in only two cases (Case 1, 7), indicating that the dynamics of bMSI in ctDNA may have a predictive value only for pathological responses[19,49], but at the same time may be used in the absence of detectable mutations. Analysis of the relationship between MSI dynamics and the development of resistance to ICI in the metastatic cases was complicated by either the loss of follow-up (Case 2) or rapid progression of disease (Case 9).

Despite the limited patient cohort, our results illuminate the promising application of MSI monitoring in the blood plasma for tracking tumor responses and disease progression in the course of ICI therapy. Analysis of bMSI in serial samples may overperform the traditional analysis of the VAF of driver mutations, and serve as a complementary approach to standard imaging studies for monitoring tumor response.

Data availability

Data will be made available from the corresponding author on reasonable request.

Received: 18 June 2024; Accepted: 23 September 2024
Published online: 08 October 2024

References

1. Keum, N. & Giovannucci, E. Global burden of colorectal cancer: Emerging trends, risk factors and prevention strategies. *Nat. Rev. Gastroenterol. Hepatol.* **16**(12), 713–732. https://doi.org/10.1038/s41575-019-0189-8 (2019).
2. Siegel, R. L. et al. Colorectal cancer statistics, 2020. *CA Cancer J. Clin.* **70**(3), 145–164. https://doi.org/10.3322/caac.21601 (2020).
3. Cornista, A. M. et al. Colorectal Cancer immunotherapy: State of the art and future directions. *Gastro Hep Adv.* **2**(8), 1103–1119. https://doi.org/10.1016/j.gastha.2023.09.007 (2023).
4. Morris, V. K. et al. Treatment of metastatic colorectal Cancer: ASCO Guideline. *J. Clin. Oncol.* **41**(3), 678–700. https://doi.org/10.1200/JCO.22.01690 (2023).
5. Koopman, M. et al. Deficient mismatch repair system in patients with sporadic advanced colorectal cancer. *Br. J. Cancer*. **100**(2), 266–273. https://doi.org/10.1038/sj.bjc.6604867 (2009).
6. Cohen, R. et al. Microsatellite instability in patients with stage III Colon cancer receiving Fluoropyrimidine with or without oxaliplatin: An ACCENT pooled analysis of 12 adjuvant trials. *J. Clin. Oncol.* **39**(6), 642–651. https://doi.org/10.1200/JCO.20.01600 (2021).
7. Ozer, M. et al. Neoadjuvant immunotherapy for patients with dMMR/MSI-High gastrointestinal cancers: a changing paradigm. *Cancers (Basel)*. **15**(15), 3833. https://doi.org/10.3390/cancers15153833 (2023). Published 2023 Jul 28.
8. Lynch, H. T. et al. Review of the Lynch syndrome: history, molecular genetics, screening, differential diagnosis, and medicolegal ramifications. *Clin. Genet.* **76**(1), 1–18. https://doi.org/10.1111/j.1399-0004.2009.01230.x (2009).
9. Luchini, C. et al. ESMO recommendations on microsatellite instability testing for immunotherapy in cancer, and its relationship with PD-1/PD-L1 expression and tumour mutational burden: A systematic review-based approach. *Ann. Oncol.* **30** (8), 1232–1243. https://doi.org/10.1093/annonc/mdz116 (2019).
10. Porkka, N. et al. Sequencing of Lynch syndrome tumors reveals the importance of epigenetic alterations. *Oncotarget*. **8**(64), 108020–108030. https://doi.org/10.18632/oncotarget.22445 (2017). Published 2017 Nov 14.
11. Kambara, T. et al. BRAF mutation is associated with DNA methylation in serrated polyps and cancers of the colorectum. *Gut*. **53**(8), 1137–1144. https://doi.org/10.1136/gut.2003.037671 (2004).
12. Weisenberger, D. J. et al. CpG island methylator phenotype underlies sporadic microsatellite instability and is tightly associated with BRAF mutation in colorectal cancer. *Nat. Genet.* **38**(7), 787–793. https://doi.org/10.1038/ng1834 (2006).
13. Alvi, M. A. et al. Molecular profiling of signet ring cell colorectal cancer provides a strong rationale for genomic targeted and immune checkpoint inhibitor therapies. *Br. J. Cancer*. **117**(2), 203–209. https://doi.org/10.1038/bjc.2017.168 (2017).
14. Venderbosch, S. et al. Mismatch repair status and BRAF mutation status in metastatic colorectal cancer patients: a pooled analysis of the CAIRO, CAIRO2, COIN, and FOCUS studies. *Clin. Cancer Res.* **20**(20), 5322–5330. https://doi.org/10.1158/1078-0432.CCR-14-0332 (2014).
15. Salem, M. et al. LBA SO-34 impact of BRAF-V600E mutation on immunologic characteristics of the tumor microenvironment (TME) and associated genomic alterations in patients with microsatellite instability-high (MSI-H) or mismatch-repair–deficient (dMMR) colorectal cancer (CRC). *Ann. Oncol.* **33**, S378. https://doi.org/10.1016/j.annonc.2022.04.441 (2022).
16. Siemanowski, J. et al. Managing difficulties of microsatellite instability testing in Endometrial Cancer-limitations and advantages of four different PCR-Based approaches. *Cancers*. **13** (6), 1268. https://doi.org/10.3390/cancers13061268 (2021).
17. Butler, T. M. et al. Exome sequencing of cell-free DNA from metastatic Cancer patients identifies clinically actionable mutations distinct from primary disease. *PLoS One*. **10** (8), e0136407. https://doi.org/10.1371/journal.pone.0136407 (2015). Published 2015 Aug 28.
18. Husain, H. & Velculescu, V. E. Cancer DNA in the circulation: The liquid biopsy. *JAMA*. **318**(13), 1272–1274. https://doi.org/10.1001/jama.2017.12131 (2017).
19. Wang, Y. et al. Utility of ctDNA in predicting response to neoadjuvant chemoradiotherapy and prognosis assessment in locally advanced rectal cancer: A prospective cohort study. *PLoS Med.* **18**(8), e1003741. https://doi.org/10.1371/journal.pmed.1003741 (2021). Published 2021 Aug 31.
20. Zhang, S. et al. Evaluation of microsatellite instability testing through cell-free DNA sequencing. *Biomarkers*. **30**(5), V35. https://doi.org/10.1093/annonc/mdz239.026 (2019).
21. Georgiadis, A. et al. Noninvasive detection of microsatellite Instability and high tumor mutation burden in cancer patients treated with PD-1 blockade. *Clin. Cancer Res.* **25**(23), 7024–7034. https://doi.org/10.1158/1078-0432.CCR-19-1372 (2019).
22. Willis, J. et al. Validation of microsatellite instability detection using a Comprehensive plasma-based genotyping panel. *Clin. Cancer Res.* **25**(23), 7035–7045. https://doi.org/10.1158/1078-0432.CCR-19-1324 (2019).

23. Yu, F., Makrigiorgos, A., Leong, K. W. & Makrigiorgos, G. M. Sensitive detection of microsatellite instability in tissues and liquid biopsies: Recent developments and updates. *Comput. Struct. Biotechnol. J.* **19**, 4931–4940. https://doi.org/10.1016/j.csbj.2021.08.037 (2021). Published 2021 Aug 27.
24. Yu, F. et al. NGS-based identification and tracing of microsatellite instability from minute amounts DNA using inter-Alu-PCR. *Nucleic Acids Res.* **49**(4), e24. https://doi.org/10.1093/nar/gkaa1175 (2021).
25. Tjulandin, S. et al. Novel PD-1 inhibitor prolgolimab: expanding non-resectable/metastatic melanoma therapy choice. *Eur. J. Cancer*. **149**, 222–232. https://doi.org/10.1016/j.ejca.2021.02.030 (2021).
26. Lebedeva, A. et al. Incidental germline findings during molecular profiling of tumor tissues for precision oncology: Molecular survey and methodological obstacles. *J. Transl Med.* **20** (1), 29. https://doi.org/10.1186/s12967-022-03230-z (2022). Published 2022 Jan 15.
27. Ivanov, M. et al. Towards standardization of next-generation sequencing of FFPE samples for clinical oncology: Intrinsic obstacles and possible solutions. *J. Transl Med.* **15** (1), 22. https://doi.org/10.1186/s12967-017-1125-8 (2017). Published 2017 Jan 31.
28. Danecek, P. et al. Twelve years of SAMtools and BCFtools. *Gigascience*. **10**(2), giab008. https://doi.org/10.1093/gigascience/giab008 (2021).
29. Garrison, E. & Marth, G. Haplotype-based variant detection from short-read sequencing. *arXiv*, arXiv:1207.3907. https://doi.org/10.48550/arXiv.1207.3907
30. McKenna, A. et al. The genome analysis Toolkit: A MapReduce framework for analyzing next-generation DNA sequencing data. *Genome Res.* **20**(9), 1297–1303. https://doi.org/10.1101/gr.107524.110 (2010).
31. Simpson, J. T. & Durbin, R. Efficient de novo assembly of large genomes using compressed data structures. *Genome Res.* **22**(3), 549–556. https://doi.org/10.1101/gr.126953.111 (2012).
32. Kockan, C. et al. SiNVICT: Ultra-sensitive detection of single nucleotide variants and indels in circulating tumour DNA. *Bioinformatics*. **33**(1), 26–34. https://doi.org/10.1093/bioinformatics/btw536 (2017).
33. Niu, B. et al. MSIsensor: Microsatellite instability detection using paired tumor-normal sequence data. *Bioinformatics*. **30** (7), 1015–1016. https://doi.org/10.1093/bioinformatics/btt755 (2014).
34. Lebedeva, A. et al. 103P MSI detection by NGS using tumor samples and liquid biopsy for patients with solid tumors: A single institution experience. *ESMO OPEN.* **8** (1), 101913. https://doi.org/10.1016/j.esmoop.2023.101913 (2023).
35. Cerami, E. et al. The cBio cancer genomics portal: an open platform for exploring multidimensional cancer genomics data [published correction appears in Cancer Discov. ;2(10):960]. *Cancer Discov*. 2012;2(5):401–404. https://doi.org/10.1158/2159-8290.CD-12-0095
36. Gao, J. et al. Integrative analysis of complex cancer genomics and clinical profiles using the cBioPortal. *Sci. Signal.* **6**(269), pl1. https://doi.org/10.1126/scisignal.2004088 (2013). Published 2013 Apr 2.
37. de Bruijn, I. et al. Analysis and visualization of longitudinal genomic and clinical data from the AACR Project GENIE Biopharma Collaborative in cBioPortal. *Cancer Res.* **83**(23), 3861–3867. https://doi.org/10.1158/0008-5472.CAN-23-0816 (2023).
38. Horak, P. et al. Standards for the classification of pathogenicity of somatic variants in cancer (oncogenicity): Joint recommendations of Clinical Genome Resource (ClinGen), Cancer Genomics Consortium (CGC), and Variant Interpretation for Cancer Consortium (VICC) [published correction appears in Genet Med. ;24(9):1991]. *Genet Med*. 24(5):986–998. (2022). https://doi.org/10.1016/j.gim.2022.01.001
39. Chakravarty, D. et al. OncoKB: A Precision Oncology Knowledge Base. *JCO Precis Oncol*. PO.17.00011 (2017). https://doi.org/10.1200/PO.17.00011
40. Patterson, S. E., Statz, C. M., Yin, T. & Mockus, S. M. Utility of the JAX Clinical Knowledgebase in capture and assessment of complex genomic cancer data. *NPJ Precis Oncol*. 3:2. Published 2019 Jan 15 (2019). https://doi.org/10.1038/s41698-018-0073-y
41. Cercek, A. et al. A comprehensive comparison of early-onset and average-onset colorectal cancers. *J. Natl. Cancer Inst.* **113**(12), 1683–1692. https://doi.org/10.1093/jnci/djab124 (2021).
42. Keller, L., Belloum, Y., Wikman, H. & Pantel, K. Clinical relevance of blood-based ctDNA analysis: Mutation detection and beyond. *Br. J. Cancer*. **124**(2), 345–358. https://doi.org/10.1038/s41416-020-01047-5 (2021).
43. Bach, S. et al. Circulating tumor DNA analysis: Clinical implications for colorectal cancer patients. A systematic review. *JNCI Cancer Spectr*. 3(3):pkz042. Published 2019 Jun 19 (2019). https://doi.org/10.1093/jncics/pkz042
44. Bettegowda, C. et al. Detection of circulating tumor DNA in early- and late-stage human malignancies. *Sci. Transl Med.* **6**(224), 224ra24. https://doi.org/10.1126/scitranslmed.3007094 (2014).
45. Bando, H. et al. Effects of metastatic sites on circulating Tumor DNA in patients with metastatic colorectal cancer. *JCO Precis Oncol.* **6**, e2100535. https://doi.org/10.1200/PO.21.00535 (2022).
46. Goldberg, S. B. et al. Early Assessment of lung cancer immunotherapy response via circulating Tumor DNA. *Clin. Cancer Res.* **24**(8), 1872–1880. https://doi.org/10.1158/1078-0432.ccr-17-1341 (2018).
47. Powles, T. et al. ctDNA guiding adjuvant immunotherapy in urothelial carcinoma. *Nature*. **595** (7867), 432–437. https://doi.org/10.1038/s41586-021-03642-9 (2021).
48. Cabel, L. et al. Circulating tumor DNA changes for early monitoring of anti-PD1 immunotherapy: a proof-of-concept study. *Ann. Oncol.* **28** (8), 1996–2001. https://doi.org/10.1093/annonc/mdx212 (2017).
49. Yue, D. et al. Circulating tumor DNA predicts neoadjuvant immunotherapy efficacy and recurrence-free survival in surgical non-small cell lung cancer patients. *Transl Lung Cancer Res.* **11** (2), 263–276. https://doi.org/10.21037/tlcr-22-106 (2022).
50. Sartore-Bianchi, A. et al. Circulating tumor DNA to guide rechallenge with panitumumab in metastatic colorectal cancer: the phase 2 CHRONOS trial. *Nat. Med.* **28**(8), 1612–1618. https://doi.org/10.1038/s41591-022-01886-0 (2022).
51. Bidard, F. C. et al. Switch to fulvestrant and palbociclib versus no switch in advanced breast cancer with rising ESR1 mutation during aromatase inhibitor and palbociclib therapy (PADA-1): A randomised, open-label, multicentre, phase 3 trial. *Lancet Oncol.* **23**(11), 1367–1377. https://doi.org/10.1016/s1470-2045(22)00555-1 (2022).
52. Lee, J. H. et al. Association between circulating tumor DNA and pseudoprogression in patients with metastatic melanoma treated with anti-programmed cell death 1 antibodies. *JAMA Oncol.* 4(5):717. (2018). https://doi.org/10.1001/jamaoncol.2017.5332
53. Chen, M. Y. & Zeng, Y. C. Pseudoprogression in lung cancer patients treated with immunotherapy. *Crit. Rev. Oncol. Hematol.* **169**, 103531. https://doi.org/10.1016/j.critrevonc.2021.103531 (2022).
54. Zulato, E., Del Bianco, P. & Nardo, G. Longitudinal liquid biopsy anticipates hyperprogression and early death in advanced non-small cell lung cancer patients treated with immune checkpoint inhibitors. *Br. J. Cancer*. **127**(11), 2034–2042. https://doi.org/10.1038/s41416-022-01978-1 (2022).
55. Jonchere, V. et al. Identification of positively and negatively selected driver gene mutations Associated with Colorectal Cancer with microsatellite instability. *Cell. Mol. Gastroenterol. Hepatol.* **6**(3), 277–300. https://doi.org/10.1016/j.jcmgh.2018.06.002 (2018).
56. Wei, J. et al. The Prognostic Value of ctDNA and bTMB on Immune Checkpoint Inhibitors in Human Cancer. *Front Oncol.* 11:706910. Published 2021 Oct 1 (2021). https://doi.org/10.3389/fonc.2021.706910
57. He, W. Z. et al. Comparison of mismatch repair status between primary and matched metastatic sites in patients with colorectal cancer. *J. Natl. Compr. Canc Netw.* **17**(10), 1174–1183. https://doi.org/10.6004/jnccn.2019.7308 (2019).

Author contributions

Olesya Kuznetsova, Daria Kravchuk, Tatiana Grigoreva, Victoria Yudina, Laima Belyaeva, and Vladislav Nikulin carried out the studies, participated in collecting data. Egor Veselovsky, Alexandra Lebedeva, Ekaterina Belova,

Anastasiia Taraskina, Alexandra Kavun, and Maxim Ivanov performed data analysis and drafted the manuscript. Alexey Tryakin, Mikhail Fedyanin, Vladislav Mileyko, and Maxim Ivanov provided administrative support. All authors contributed to manuscript revision, read, and approved the submitted version.

Funding
This study was supported by the Russian Science Foundation (grant No. 22-75-10154, https://rscf.ru/project/22-75-10154/).

Declarations

Competing interests
Egor Veselovsky, Alexandra Lebedeva, Olesya Kuznetsova, Ekaterina Belova, Anastasia Taraskina, Tatyana Grigoreva, Alexandra Kavun, Laima Belyaeva, Vladislav Mileyko, Maxim Ivanov are currently employed by OncoAtlas LLC. Other co-authors have no conflicts of interest to disclose.

Additional information
Supplementary Information The online version contains supplementary material available at https://doi.org/10.1038/s41598-024-73952-1.

Correspondence and requests for materials should be addressed to M.I.

Reprints and permissions information is available at www.nature.com/reprints.

Publisher's note Springer Nature remains neutral with regard to jurisdictional claims in published maps and institutional affiliations.